Topological Changes in Bipolar Nematic Droplets under Flow

A. Fernández-Nieves,[1,2] D. R. Link,[1] M. Márquez,[2,3] and D. A. Weitz[1]

[1]*Department of Physics and HSEAS, Harvard University, Cambridge, Massachusetts 02138, USA*

[2]*Interdisciplinary Network of Emerging Science and Technology (INEST) Group, Research Center, Phillip Morris USA, Richmond, Virginia 23298, USA*

[3]*Harrington Department of Bioengineering, Arizona State University, Tempe, Arizona 85287, USA*

(Received 28 August 2006; revised manuscript received 22 November 2006; published 21 February 2007)

Bipolar liquid crystal drops moving inside microchannels exhibit periodic director field transformations due to induced circulating flows inside them. These modifications are characterized by changes in the type of point surface disclinations; they periodically change from splay to bend disclinations, implying the drop changes between bipolar and escaped concentric configurations. Upon stopping the flow, this structure does not relax to the lower energy bipolar configuration; we argue this is due to drop flattening inside the channels.

DOI: 10.1103/PhysRevLett.98.087801 PACS numbers: 61.30.−v, 47.55.D−, 47.61.−k, 77.84.Nh

Nematic liquid crystals are characterized by their director field, **n**, which can be visualized by using polarized microscopy. When the system is confined, boundary conditions impose unavoidable topological constraints on the director field and typically result in one or more disclinations, which are singular regions about which the director rotates through multiples of π radians. Energetic considerations finally determine the final ground state of the system; any nonuniformity in **n** can increase the free energy as characterized by the Frank free energy density [1]. The system is driven to a specific configuration that minimizes the free energy while complying with the topological constraints imposed by the boundaries.

The topology of a sphere of nematic liquid crystal depends critically on the nature of the boundary conditions: if the boundary conditions are homeotropic, so **n** is normal to the surface, radial [Fig. 1(a)] and axial [Fig. 1(b)] configurations are allowed. By contrast, if the boundary conditions are parallel, so **n** is along the surface, bipolar [Fig. 1(c)] and concentric [Fig. 1(d)] configurations are allowed. Even more complex structures are also possible, although these incorporate other distortions to the director field. For planar anchoring the bipolar configuration is most typically observed; this is the case in opto-electronic applications such as polymer dispersed liquid crystals and their three-dimensional holographic counterparts [2–4]. Bipolar droplets have **n** aligned, on average, between two splay-type surface disclinations whose strength or surface topological charge is $s = +1$; this is determined by the rotation of the director field about the core. This satisfies the requirements of the Poincaré theorem [5], that the total topological charge on the surface of a sphere is $s_{\text{total}} = +2$. By contrast, the concentric configuration in Fig. 1(d) is typically not observed as its structure normally evolves to a lower energy configuration that relaxes the presence of the disclination line by allowing **n** to twist and leave the plane; this is often called an escape into the third dimension [6] [Fig. 1(e)]. The escaped concentric structure also has two $s = +1$ surface defects, but these are bend disclinations.

Transformation between the different configurations can be accomplished by changing the surface boundary conditions [7,8] or by forcing the alignment of the director field while maintaining the boundary conditions unaltered [9–13]. The escaped concentric configuration can be easily transformed into a bipolar configuration; for example, application of electric fields aligns **n** in the direction of the field and both orients a bipolar configuration and transforms a escaped concentric into a bipolar configuration. Once transformed, the bipolar configuration does not revert back to the escaped concentric as there is a significant energy barrier between them [2,11,14]. This reflects the high degree of symmetry of the bipolar configuration. Indeed, it is virtually impossible to transform the bipolar configuration into any other allowable configuration while preserving the requisite boundary conditions.

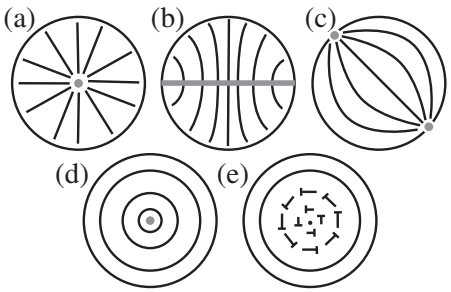

FIG. 1. Examples of nematic liquid crystal drops. For normal surface anchoring: (a) radial and (b) axial configurations; these are characterized, respectively, by a point defect at the sphere center and a disclination line along the drop equator. For planar anchoring at the drop surface: (c) bipolar, (d) concentric, and (e) escaped concentric configurations. The bipolar drop possesses two diametrically opposed splay-type point disclinations on the surface. The concentric drop possesses a disclination line through the sphere center; this configuration is usually not observed, as it is energetically favorable for the line defect to escape in the third dimension. The result is the escaped concentric structure that has two diametrically opposed bend-type point disclinations on the surface.

In this Letter, we introduce a new method to induce topological changes in the droplet configurations allowing us to transform reversibly between bipolar and escaped concentric. We show that flow of liquid crystal droplets in a continuous fluid and confined in a thin channel induces the transformation of the topological defects leading to the changes in configuration. We show that, despite the strong repulsion between them, the two point defects join and separate cyclically and when doing so, the splay defects change to bend defects. The drop thus periodically changes between bipolar and escaped concentric. Upon stopping the flow, drops in the escaped concentric configuration remain as such, even though $K_{\text{bend}} > K_{\text{splay}}$ for our liquid crystal, thus implying this structure has higher energy than the bipolar [2,14]. The periodic transition from bipolar to escaped concentric thus allows stabilization of higher energy nematic configurations that would otherwise be unattainable.

Monodisperse emulsions are prepared by extrusion of penthylcyanobiphenyl (5CB), a nematic liquid crystal, through a thin capillary (3–10 μm in diameter) into coflowing water containing 1 wt% polyvinyl alcohol (PVA) [15]. The PVA leads to parallel boundary conditions for **n** at the drop surface resulting in a drop with a bipolar configuration, since K_{splay} is less than K_{bend} for 5CB [16]. An example of nematic drops with diameter $d = 30$ μm is shown in Fig. 2(a). These are introduced into a channel fabricated by soft-lithographic techniques [17], and having a width and height equal to 100 and 10 μm, respectively [Fig. 2(b)]. As a result, the drops are constrained upon entering the channel; this allows precise visualization of the textures using optical microscopy and crossed polarizers. We emphasize that although the droplets are not spherical, their interface remains smooth due to surface tension. A thin water film separates the liquid crystal from the confining channel walls as is typical for bubbles and droplets flowing in confined geometries [18]. When the emulsion is pumped through the channel the relative motion between the flowing outer fluid and the internal liquid crystal induces flow within the droplet,

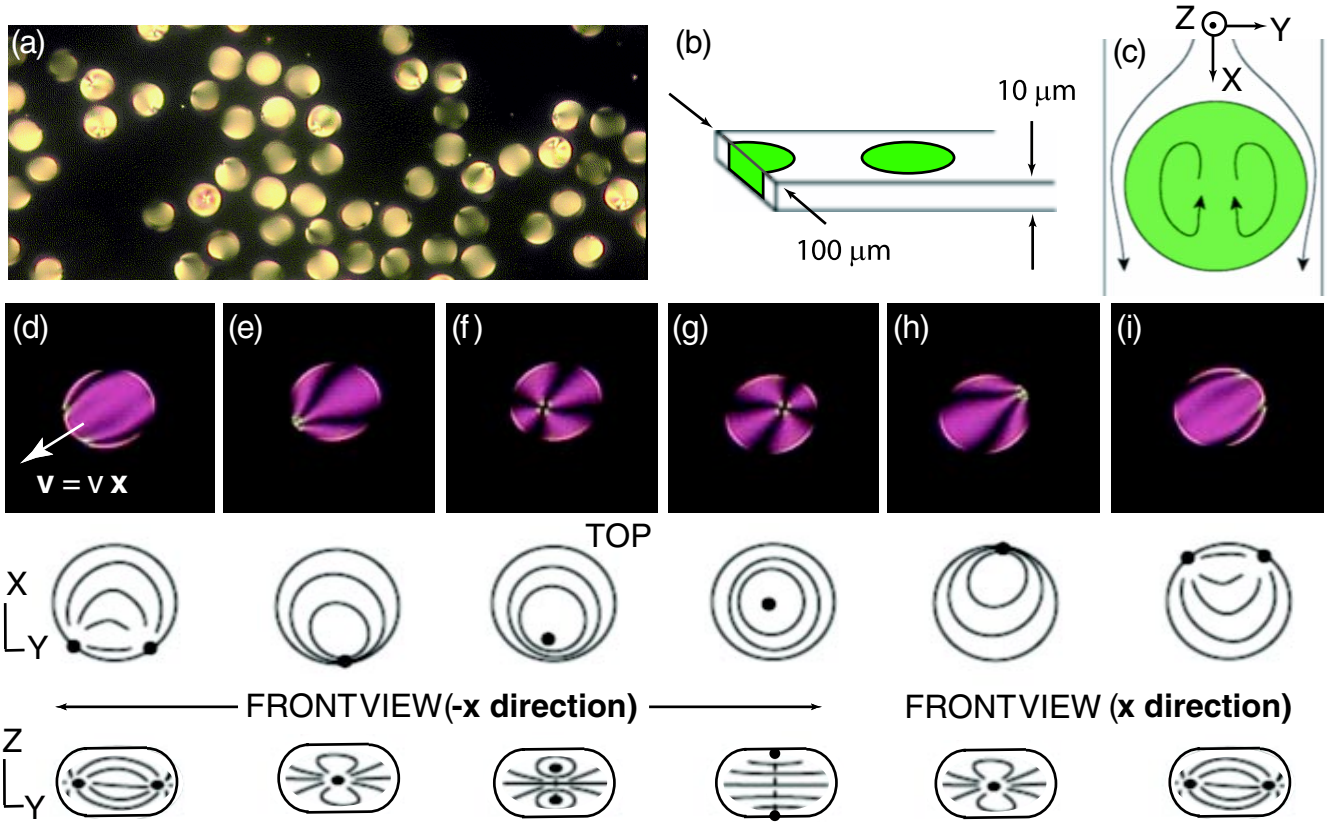

FIG. 2 (color online). (a) Cross-polarized image of the liquid crystal (LC) emulsion. The drops are bipolar and have a diameter $d = 30$ μm. (b) Schematics of the drops inside a 100×10 μm^2 channel. (c) Velocity flow lines inside and outside the drops. (d)–(i) Cross-polarized images of a moving drop. The motion direction is indicated by the velocity vector in (d). Circulation flows inside the drop causes the disclinations to move along the drop equator (d), meet at the drop front (e), return through the drop top and bottom (f), (g), meet again at the drop back (h), and move along the equator again (i). The images show the tentative director field configuration depicted as top and side views in the lower set of figures. Our interpretation suggests that the defects are $s = +1$ splay-type while moving along the drop equator. They form a $s = +2$ disclination at the front and back of the drop and are bend-type $s = +1$ point defects when moving though the drop top and bottom. Our interpretation implies that the drop changes cyclically between bipolar and escaped concentric configurations.

shown schematically in Fig. 2(c). This further allows relative motion between the drops and the surrounding liquid to be achieved by simply pumping the emulsion through the channel. Typical drop velocities are $v \simeq 20\ \mu\mathrm{m/s}$.

The internal flow of the liquid crystal drop results in dramatic configurational changes, as illustrated by the optical micrographs, taken with crossed polarizers, showing the time evolution of a single drop, Figs. 2(d)–2(i). From these pictures, we suggest a tentative orientation for the nematogens and for the resultant topology of the defects; these are shown schematically, in top and side views, in the lower set of figures in Fig. 2. The drop begins with a bipolar structure aligned along the direction of flow; the internal circulation initially brings the two boojums closer together at the front of the drop, as shown in Fig. 2(d). The flow then forces the two boojums to merge into a single defect with a topological strength of $s = +2$, as shown in Fig. 2(e). Since the two defects repel one another with a force that varies inversely with their separation, this requires a very strong force, which is exerted by the flow of the liquid crystal. The single defect then breaks into two separate $s = +1$ defects which subsequently move apart towards the top and bottom of the drop, as shown in Figs. 2(f) and 2(g). We hypothesize that these $s = +1$ defects are in fact bend defects and that at this point the drop has attained the escaped concentric configuration. This is driven strictly by the induced flow of the nematic liquid crystal. Further flow draws the two bend defects towards the back of the drop where they join again forming a single $s = +2$ defect, Fig. 2(h). This defect is again broken into two separate defects, each being $s = +1$ splay defects, Fig. 2(f). These defects are pulled apart by the flow and the drop achieves a bipolar configuration, whereupon it starts the evolution again. This sequence of topological transformations is repeated continuously and periodically as long as the flow is continuous. Throughout all of these transformations, the total topological charge of all the surface defects remains constant at $s_{\mathrm{total}} = +2$, as required by the Poincaré theorem.

To verify that the drop indeed attains the escaped concentric configuration, we confirm the bend character of the $s = +1$ defects shown in Figs. 2(f) and 2(g) by using a birefringent plate whose optical axis is placed along one of the bright sections of the crosslike structure seen in Figs. 2(f) and 2(g). We then compare the colors in the resultant images to those on a Michel-Levy chart [19]. For a splay-type defect, we expect the birefringence to be larger along the optic axis of the birefringent plate, as shown schematically in Figs. 3(a) and 3(b). By contrast, for a bend-type defect, we expect the birefringence to be larger in the direction perpendicular to the optic axis of the birefringent plate, as shown schematically in Figs. 3(a) and 3(c). By comparing the colors of three typical drops [Figs. 3(d)–3(f)] to those on the Michel-Levy chart, Fig. 3(g), we see that the birefringence is greater in the direction perpendicular to the plate optic axis; indeed, for all drops in this configuration, we invariably see the bend-type defects. This confirms that the structure of the drops is indeed escaped concentric [20]. These flow induced transformations are the only example of which we are aware that allow the formation of an escaped concentric configuration for a nematic whose bend elastic constant is greater than the splay elastic constant.

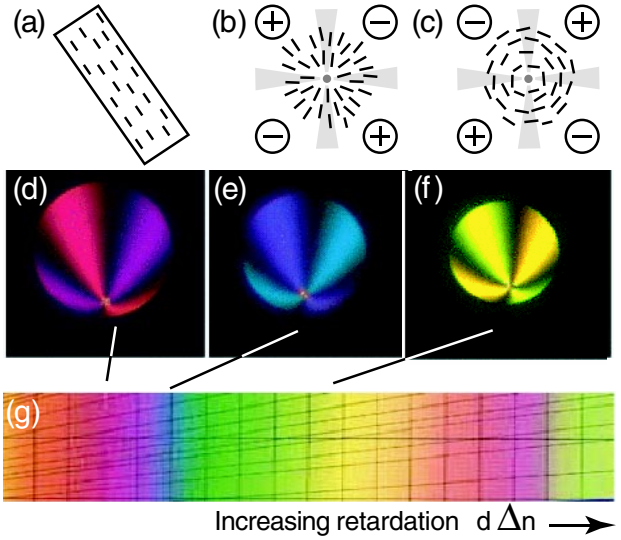

FIG. 3 (color online). (a) Schematic representation of a birefringent plate with its optic axis along its longitudinal direction. (b)–(c) Schematics of splay (b) and bend (c) $s = +1$ point defects. When placed on top of the birefringent plate and observed between crossed polarizers, birefringence will add in regions where the director and the plate optic axis are parallel and will subtract in regions where both are perpendicular; this is indicated with the plus and minus signs in the defect schematics. (d)–(f) Three typical drops constrained in channel regions of different height. By comparing the observed colors to those on the Michel-Levy chart (g), we see that the birefringence is greater in the direction perpendicular to the plate optic axis. This implies that the defects have a bend character and the drop is escaped concentric.

Surprisingly, when the drops are in the escaped concentric configuration and the flow is stopped, they retain their structure; they do not spontaneously return to the bipolar structure even though its energy is lower because

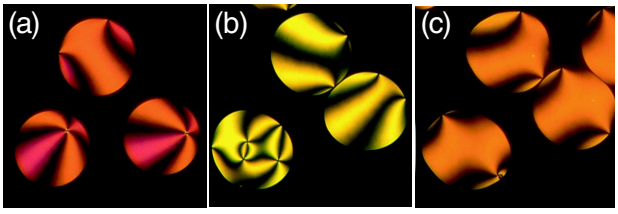

FIG. 4 (color online). Escaped concentric to bipolar transition after heating the liquid crystal to the isotropic phase and cooling back to the nematic phase. (a) Coexisting bipolar and escaped concentric drops before this transition. (b) Transient regime after cooling back to the nematic phase where defects are created and annihilated. (c) Final bipolar drop configuration.

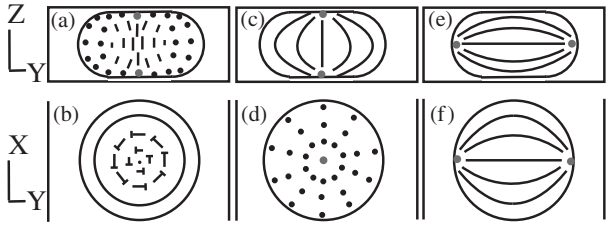

FIG. 5. Front and top views of a flattened pancakelike drop inside the channel illustrating the presence of a high energy barrier that prevents the transition from the escaped concentric configuration to the lower energy bipolar configuration. Points indicate that **n** is perpendicular to the plane. (a), (b) Escaped concentric configuration. (c), (d) Intermediate highly bent configuration. (e), (f) Bipolar configuration.

$K_{\mathrm{bend}}/K_{\mathrm{splay}} > 1$ [14]. It is conceivable that the flow of the fluid has aligned the PVA at the droplet interface which would prevent the director from rearranging, thereby maintaining the escaped concentric configuration. To test this possibility, we heat the nematic to the isotropic phase; upon cooling, drops initially in the escaped concentric configuration [Fig. 4(a)] undergo a transient regime, in which defects are created and annihilated [Fig. 4(b)], but then revert to the lowest energy bipolar structure [Fig. 4(c)]. This result shows that shear alignment of the polymer at the interface is not the underlying cause of the stabilization of the escaped concentric configuration. Instead, we believe that the stability of the escaped concentric configuration results from the existence of an energy barrier between this structure and the lower energy bipolar configuration; this prevents the spontaneous transition between these two structures. We believe that the origin of this energy barrier is the highly deformed shape of the droplet in the narrow channel; because the height of the channel is so much smaller than that of the diameter of the drop, its shape is highly compressed into a pancakelike structure, as shown schematically in Fig. 2(b). In this case, the transition from the escaped concentric configuration, shown schematically in Fig. 5(a) and 5(b), to the bipolar configuration, shown schematically in Fig. 5(e) and 5(f), must pass through an intermediate configuration, shown in Fig. 5(c) and 5(d). This intermediate configuration is much higher in energy because the structure is highly bent. The resultant energy barrier stabilizes the escaped concentric configuration.

These results demonstrate a novel mean of transforming defect configurations in drops. The large forces induced by the flow of the fluid overcome the significant barrier in energy and results in formation of structures that have been otherwise elusive. This is the only method available to create escaped concentric drops from bipolar drops using a liquid crystal that otherwise does not produce them.

We acknowledge discussions with M. Nakata and R. B. Meyer. This work was supported by NASA (No. NAG3-2381) and by the NSF (No. DMR-0602684) and the Harvard MRSEC (No. DMR-0213805). A. F.-N. is grateful to Ministerio de Ciencia y Tecnología (No. MAT2004-03581) and to University of Almeria (leave of absence).

[1] P. G. de Gennes and J. Prost, *The Physics of Liquid Crystals* (Oxford University Press, New York, 1995).
[2] P. S. Drzaic, *Liquid Crystal Dispersions* (World Scientific, Singapore, 1995).
[3] R. L. Sutherland, V. P. Tondiglia, L. V. Natarajan, T. J. Bunning, and W. W. Adams, Appl. Phys. Lett. **64**, 1074 (1994); T. J. Bunning, L. V. Natarajan, V. P. Tondiglia, and R. L. Sutherland, Annu. Rev. Mater. Sci. **30**, 83 (2000).
[4] D. Rudhardt, A. Fernández-Nieves, D. R. Link, and D. A. Weitz, Appl. Phys. Lett. **82**, 2610 (2003).
[5] M. Kleman, O. D. Lavrentovich, and Y. A. Nastishin, in *Dislocations and Disclinations in Mesomorphic Phases*, edited by F. R. N. Nabarro and J. P. Hirth, Dislocations in Solids Vol. 12 (Elsevier, New York, 2004).
[6] C. Williams, P. Pieranski, and P. E. Cladis, Phys. Rev. Lett. **29**, 90 (1972); P. E. Cladis and M. Kleman, J. Phys. (France) **33**, 39 (1972); R. B. Meyer, Philos. Mag. **27**, 405 (1973).
[7] O. D. Lavrentovich, Liq. Cryst. **24**, 117 (1998); G. E. Volovik and O. D. Lavrentovich, Sov. Phys. JETP **58**, 1159 (1984).
[8] O. O. Prischepa, A. V. Shabanov, and V. Ya. Zyryanov, JETP Lett. **79**, 257 (2004); O. O. Prishchepa, A. V. Shabanov, and V. Ya. Zyryanov, Phys. Rev. E **72**, 031712 (2005).
[9] J. H. Erdmann, S. Zumer, and J. W. Doane, Phys. Rev. Lett. **64**, 1907 (1990).
[10] F. Xu, H. S. Kitzerow, and P. P. Crooker, Phys. Rev. A **46**, 6535 (1992).
[11] F. Xu, H. S. Kitzerow, and P. P. Crooker, Phys. Rev. E **49**, 3061 (1994).
[12] A. V. Kovalchuk, M. V. Kurik, O. D. Lavrentovich, and V. V. Sergan, Sov. Phys. JETP **67**, 1065 (1988).
[13] V. G. Bodnar, O. D. Lavrentovich, and V. M. Pergamenshchik, Sov. Phys. JETP **74**, 60 (1992).
[14] P. S. Drzaic, Mol. Cryst. Liq. Cryst. **154**, 289 (1988); Liq. Cryst. **26**, 623 (1999).
[15] P. B. Umbanhowar, V. Prasad, and D. A. Weitz, Langmuir **16**, 347 (2000).
[16] H. Stark, Phys. Rep. **351**, 387 (2001).
[17] J. C. McDonald *et al.*, Electrophoresis **21**, 27 (2000).
[18] F. P. Bretherton, J. Fluid Mech. **10**, 166 (1961).
[19] P. Kerr, *Optical Mineralogy* (McGraw-Hill, New York, 1977).
[20] We further note that the stability criterion of Williams [21] for the formation of a twisted bipolar configuration is not fulfilled. Indeed, for 5CB, $K_{\mathrm{splay}} \neq K_{\mathrm{twist}} + 0.431 K_{\mathrm{bend}}$. This supports our observation of an escaped concentric drop.
[21] R. D. Williams, J. Phys. A **19**, 3211 (1986).